

NJC

Accepted Manuscript



This article can be cited before page numbers have been issued, to do this please use: S. Hasanzadeh Banakar, M. G. Dekamin and A. Yaghoubi, *New J. Chem.*, 2018, DOI: 10.1039/C8NJ01053F.



This is an Accepted Manuscript, which has been through the Royal Society of Chemistry peer review process and has been accepted for publication.

Accepted Manuscripts are published online shortly after acceptance, before technical editing, formatting and proof reading. Using this free service, authors can make their results available to the community, in citable form, before we publish the edited article. We will replace this Accepted Manuscript with the edited and formatted Advance Article as soon as it is available.

You can find more information about Accepted Manuscripts in the [author guidelines](#).

Please note that technical editing may introduce minor changes to the text and/or graphics, which may alter content. The journal's standard [Terms & Conditions](#) and the ethical guidelines, outlined in our [author and reviewer resource centre](#), still apply. In no event shall the Royal Society of Chemistry be held responsible for any errors or omissions in this Accepted Manuscript or any consequences arising from the use of any information it contains.



New J. Chem.

ARTICLE

Selective and highly efficient synthesis of xanthenedione or tetraketone derivatives catalyzed by ZnO nanorods decorated graphene oxide

Received 00th January 20xx,
Accepted 00th January 20xx

DOI: 10.1039/x0xx00000x

www.rsc.org/

Sepideh Hasanzadeh Banakar, Mohammad G. Dekamin* and Amene Yaghoubi

ZnO nanorods decorated graphene oxide (GO/ZnO), having Bronsted and Lewis acid centers, was introduced as a selective, highly efficient and recoverable nanocatalyst for the pseudo three-component synthesis of diverse tetraketone or xanthenedione derivatives *via* condensation of aromatic aldehydes with 1,3-dicarbonyl compounds in short reaction times and good to excellent yields in H₂O under refluxing and solvent-free conditions, respectively. Moreover, the GO/ZnO nanocomposite was recovered and reused at least four times without significant decrease in its activity. Low loading of the catalyst, high to excellent yields, eliminating of any toxic heavy metals or corrosive reagents for modification of the catalyst, simple separation and purification of the products, and reusability of the catalyst are the most significant advantages of this green protocol.

Introduction

In recent years, nanoscience has emerged as an attractive and important research area among chemistry, material, physics, medicinal, biology, mechanic and other sciences because of its novel, extensive and unique applications in various fields. Hence, a lot of studies have been focused onto nanoparticles. Their reactivity, toughness and other properties are also dependent on their unique size, shape and structure.¹ Indeed, nanoparticle chemistry is a new branch of chemical research. For more than a century, transition metal particles were widely used as heterogeneous catalysts.² Today, nanoscience appears to be essential and important in catalysis of various reactions, especially in organic chemistry. Nanocatalysts have been used in various reactions especially multicomponent reactions to enhance the yield of products in shorter reaction times and easier separation and recovery.³ Therefore, development of eco-friendly methods for the preparation of nanoparticles is an important branch of nanotechnology.^{4,5}

The fabrication of graphene oxide-based nanocomposite materials have been performed by different methods or techniques such as hydrothermal, electrochemical deposition, *in situ* polymerization, sol-gel, sonochemical, electrospinning, microwave and photocatalysis.⁶ However, finding a more appropriate way to prepare this type of nanocomposites is still a great challenge.

Graphene oxide (GO) contains a range of reactive oxygen functional groups. GO consists of intact graphitic regions interspersed with sp³-hybridized carbons containing functional groups such as carboxyl, hydroxyl, and epoxide on the edge, top, and bottom of surface of each sheet.⁷⁻¹⁰ Furthermore, owing to its unique properties such as thermal, chemical and mechanical stability, high specific surface area and strong interactions with metal clusters,¹¹ potential applications of graphene and GO have been actively pursued in the different fields. For example, biological applications for cellular imaging, drug delivery,¹² and bio sensing,¹³ nano electronics as well as nanocomposites¹⁴ have been reported in recent years. Furthermore, GO is a promising material for the catalytic applications.¹⁵

Catalysts are an important issue in the synthesis of fine chemicals, production of bulk chemicals and environmental industries.¹⁶ Therefore, utilization of catalysts with appropriate properties including ease of preparation, recoverability, recyclability, and higher yields of the desired products is the most important aims in the catalyst-design science. Zinc oxide (ZnO) is an inexpensive, air- and moisture stable, reusable, commercially available and environmentally benign material. ZnO demonstrates semiconducting, piezoelectric, and pyroelectric multiple properties.¹⁷⁻²¹ Many nanostructures of ZnO have been prepared under specific growth conditions, such as nanocombs, nanorings, nanohelices/nanosprings, nanobows, nanobelts, nanowires, nanocages, nanocolumnar and nanorods.²²⁻²⁵ Hence, ZnO is probably the richest family of nanostructures among all materials which has been used as catalyst.^{22, 26-30} Indeed, ZnO nanoparticles decorated graphene oxide (GO/ZnO) provide combination of ZnO and GO properties in which the catalytic activity of each part has been improved. However, only a few metal oxide or metal nanoparticles-graphene (or graphene oxide) hybrids have been reported and fewer

Pharmaceutical and Heterocyclic Compounds Research Laboratory, Department of Chemistry, Iran University of Science and Technology, Tehran, 16846-13114, Iran.
Email: mdekamin@iust.ac.ir

Electronic Supplementary Information (ESI) available: [details of any supplementary information available should be included here]. See DOI: 10.1039/x0xx00000x

ARTICLE

New J. Chem.

studies have investigated their potent applications in different fields. Some recently applications of GO/ZnO, as a stable nanocomposite, include synthesis of 5-substituted-1*H*-tetrazoles,³¹ chemical gas sensors,³² photocatalytic activities,³³ photovoltaic cells,³⁴ tunable fluorescence³⁵ and simultaneous detection and degradation of harmful organic contaminants from aqueous solution.³⁶

Tetraketones (2,2'-arylmethylene bis(3-hydroxy-5,5-dimethyl-2-cyclohexene-1-one)) and xanthenediones (1,8-dioxo-octahydroxanthene) derivatives are important classes of oxygen-containing organic compounds that have gained much attention due to their numerous applications in pharmacy, biology and material science. Tetraketone derivatives demonstrate biological and therapeutic properties such as lipoxygenase inhibitory (compound **A**),³⁷ tyrosinase inhibitory (compound **B**)^{38, 39} and anti-tubercular (compound **C**)⁴⁰ activities as well as selective estrogen receptor modulators treatment of breast cancer (compound **D**) (Fig. 1).⁴¹ Furthermore, they are important synthetic intermediates that can serve as versatile precursors in the synthesis of xanthenes and polyhydroacridine derivatives.⁴² On the other hand, xanthene-based compounds are organic fluorophores and demonstrate fluorescence properties such as fluorescein and rhodamine.⁴³

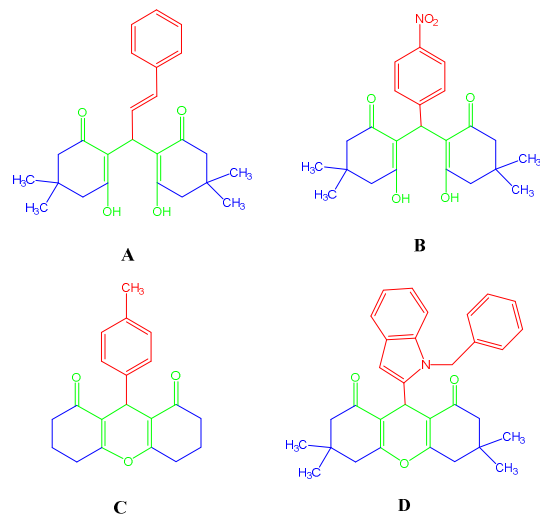


Fig. 1 Selected examples of 2,2'-arylmethylene bis(3-hydroxy-5,5-dimethyl-2-cyclohexene-1-one) and 1,8-dioxo-octahydroxanthene derivatives demonstrating biological and pharmacological activity.

Recently, various homogeneous and heterogeneous catalysts have been used in expanding and improving of reaction conditions for the synthesis of tetraketone and xanthenedione derivatives. Some recent catalytic systems are nickel nanoparticles,⁴⁴ nanocrystalline TiO₂,⁴⁵ copper nanoparticles supported onto silica,⁴⁶ [n-Pr₂NH₂][HSO₄],⁴⁷ molybdate sulfonic acid,⁴⁸ BiOCl,⁴⁹ CsF,⁵⁰ natural phosphate,⁵¹ Amano lipase DF,⁵² β-cyclodextrin grafted with butyl sulfonic acid,⁵³ MCM-41-SO₃H,⁵⁴ [MNP-PIm-SO₃H]Cl,⁵⁵ Cs_{2.5}H_{0.5}PW₁₂O₄₀,⁵⁶ Fe₃O₄@SiO₂-imid-PMA,⁵⁷ amino-appended β-cyclodextrin,⁵⁸ CoFe₂O₄ nanoparticles,⁵⁹ ZnO particles,^{29, 60} GO-SO₃H⁶¹ and urea under ultrasonication.⁶² Most of these synthetic strategies suffer from restrictions such as harsh reaction conditions, long reaction times, toxicity of solvents, often expensive catalysts

which are not recoverable, and production of by-products. In continuation of our interest to develop mild, green and efficient heterogeneous catalysts for different MCRs,⁶³⁻⁷³ we wish herein to report the catalytic activity of the graphene oxide/ZnO nanocomposite (GO/ZnO, **1**, Fig. 2), as a green, novel, recoverable and highly efficient heterogeneous nanocatalyst for the one-pot pseudo three-component synthesis of different tetraketones in water, as a green solvent, as well as preparation of xanthenedione derivatives under solvent-free conditions (Scheme 1).

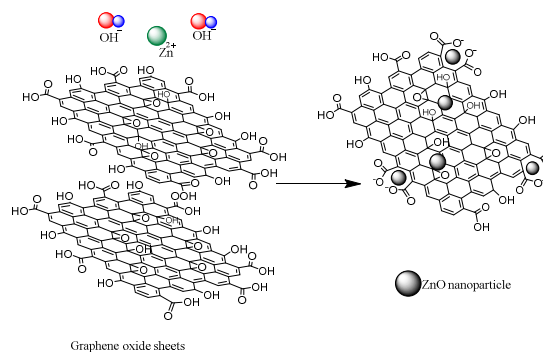
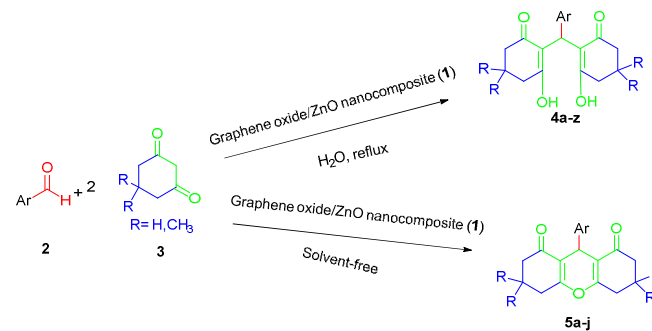


Fig. 2 A schematic structure of the ZnO nanorods decorated graphene oxide (GO/ZnO) nanocomposite (**1**).



Scheme 1. One-pot pseudo three-component synthesis of 2,2'-arylmethylene bis(3-hydroxy-5,5-dimethyl-2-cyclohexene-1-one)s (**4a-z**) and 1,8-dioxo-octahydroxanthenes (**5a-j**) catalyzed by GO/ZnO (**1**).

Results and discussion

The graphene oxide (GO) was first prepared according to reported procedures in literature with a slight modification.⁷⁴ After that, GO/ZnO nanocomposite (**1**) was prepared by functionalizing of GO with Zn(OAc)₂·2H₂O analogous with described procedure by Nasrollahzadeh and coworkers³¹ with a slight modification. In the preliminary studies, various mass ratios of GO to Zn(OAc)₂·2H₂O such as 1:3, 1:2 and 1:1 were examined for the preparation of GO/ZnO nanocomposite (**1**). Indeed, the best result was obtained by 1:1 mass ratio of GO and Zn(OAc)₂·2H₂O. Subsequently, the obtained materials were characterized with several spectroscopic and techniques such as Fourier transform infrared (FTIR) spectroscopy, field emission

scanning electron microscopy (FESEM), energy dispersive X-ray spectroscopy (EDX) and thermogravimetric analysis (TGA) and powder X-ray diffraction (XRD). The reaction between GO and ZnO nanoparticles under ultrasound and then formation of ZnO nanoparticles (in the presence of OH⁻) on graphene oxide sheets and preparation of GO/ZnO nanocomposite (**1**) are shown in (Fig. 2).

The FTIR spectra of the GO/ZnO nanocomposite (**1**) and GO are compared in Fig. 3. The observed changes are referred to chemical interactions between functional groups of GO and ZnO. In the FTIR spectrum of GO, the appeared characteristic bands at 1724, 1616 and 1200 cm⁻¹ were assigned to C=O, C=C and C-OH functional groups, respectively. Moreover, the signals observed at 1053 and 835 cm⁻¹ are attributed to epoxy (C-O-C) vibrations. On the other hand, in the FTIR spectrum of GO/ZnO nanocomposite (**1**), the strong absorption bands in

the range of < 500 cm⁻¹ such as observed signals at 414, 443 cm⁻¹ are assigned to the stretching vibrations of the Zn-O-Zn interactions.⁷⁵ Interestingly, the characteristic carbonyl signal of GO at 1724 cm⁻¹ has almost been disappeared in the GO/ZnO nanocomposite. This observation as well as absence of a very broad band of COOH functional groups in the region 3300-2400 cm⁻¹ confirm that ZnO nanoparticles are completely bonded with the formed carboxylates at the edge of GO. However, the observed broad characteristic bands at 3600-3300 are attributed to the stretching vibration of the O-H bonds of COH groups on the surface of GO/ZnO nanocomposite (**1**). Indeed, FTIR spectrum of GO/ZnO nanomaterial (**1**) shows the presence of the ZnO characteristic bands and reduction in peak intensity of the band corresponding to carboxylic acid (2400-3600 cm⁻¹). All these findings confirm functionalization of GO by ZnO (Figs. 2, 3).

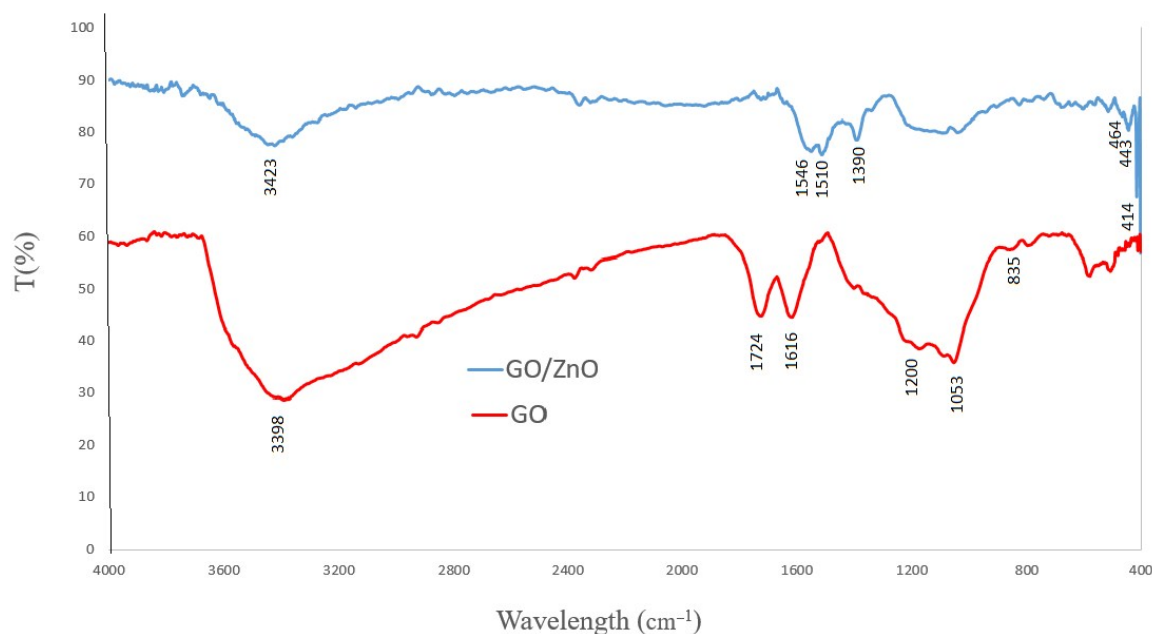


Fig. 3 FTIR spectra of the graphene oxide (GO) sheets (down) and ZnO decorated graphene oxide (GO/ZnO) nanocomposite (**1**, up).

Furthermore, energy dispersive X-ray spectroscopy (EDX) of GO/ZnO nanocomposite (**1**) indicates the presence of C, O and Zn elements in the nanomaterial composition. These observations, especially presence of Zn in the composition of the GO/ZnO nanomaterial (**1**) illustrates the successful inclusion of expected ZnO in the material network (Fig. 4).

On the other hand, the morphology and particle size of the GO/ZnO nanocomposite (**1**) was evaluated using field emission scanning electron microscopy (FESEM). As it can be clearly seen in Figure 5, the FESEM images show GO layers (Fig. 5b) and immobilized ZnO nanoparticles on the surface or between graphene oxide layers (Fig. 5a). The gray thin films are the GO sheets and the white regions on the GO background demonstrate the presence of ZnO nanorods. Moreover, X-ray diffraction patterns (XRD) of GO, ZnO and GO/ZnO

nanocomposites (**1**) are outlined in Figure 6. The Existence of GO signal at $2\theta = 12.12^{\circ}$ ³³ and other diffraction peaks in the structure of GO/ZnO nanocomposite (**1**) which are similar to pure hexagonal phase of ZnO nanorods (JPCDS 36-1451)^{22, 31} confirm construction of this nanocomposite.

The thermal stability of the GO/ZnO nanocomposite (**1**) was also investigated using thermogravimetric analysis (TGA) technique (See ESI). This analysis illustrated higher thermal stability of GO/ZnO nanocomposite (**1**) than GO. A weight loss at the temperature below 200 °C corresponding to the removal of water. On the other hand, the second weight loss between 200 and 400 °C is attributed to desorption of oxygenated carbon groups located in the GO/ZnO nanocomposite (**1**) structure.

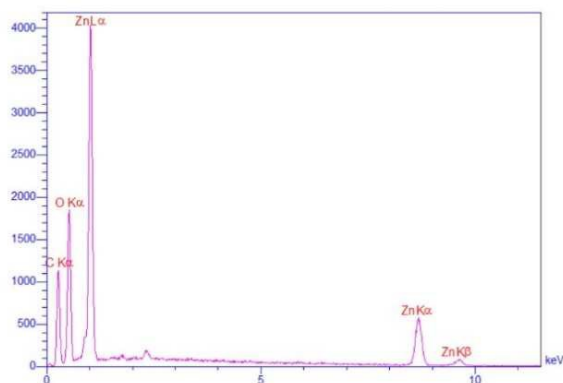


Fig. 4. Energy dispersive spectroscopy (EDX) pattern of the ZnO decorated graphene oxide (GO/ZnO) nanocomposite (1).

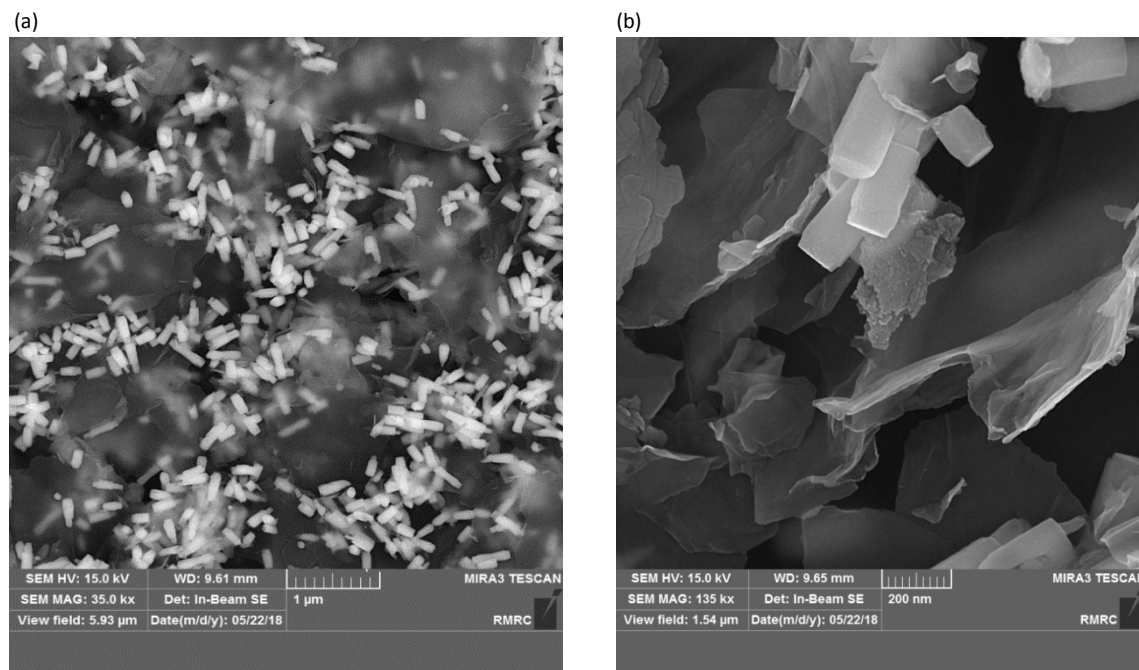


Fig. 5. Field emission scanning electron microscopy (FESEM) of the ZnO nanorods-decorated graphene oxide (GO/ZnO) nanocomposite (a, b).

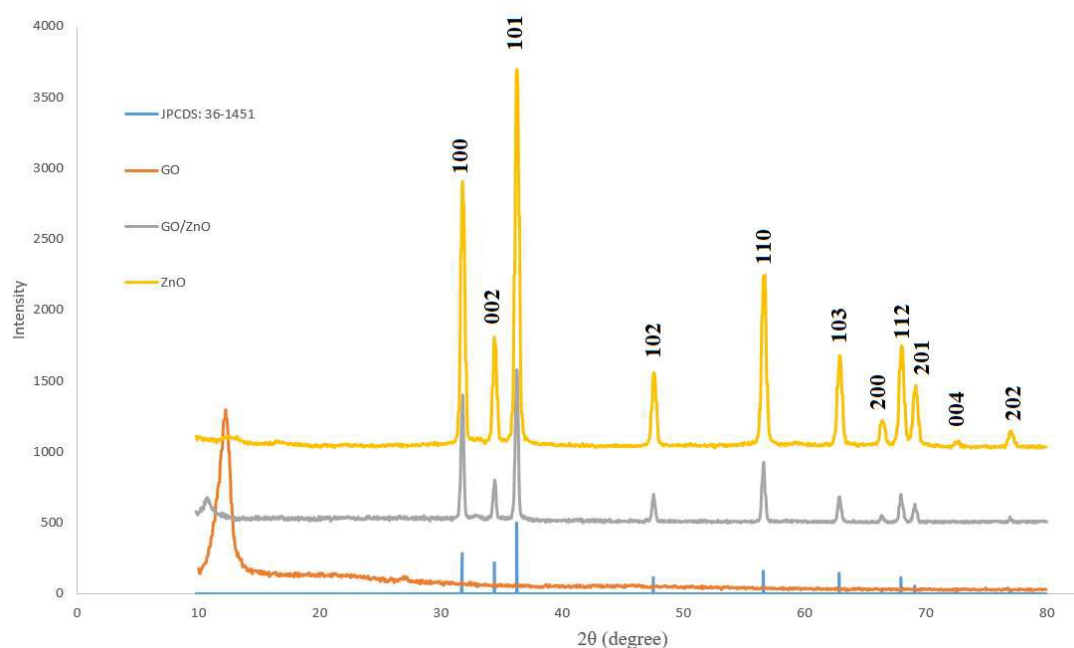


Fig. 6. X-Ray diffraction (XRD) pattern of the GO, ZnO nanorods-decorated graphene oxide (GO/ZnO) nanocomposite (**1**), ZnO nanoparticles and the hexagonal phase of ZnO (JPCDS 36-1451).

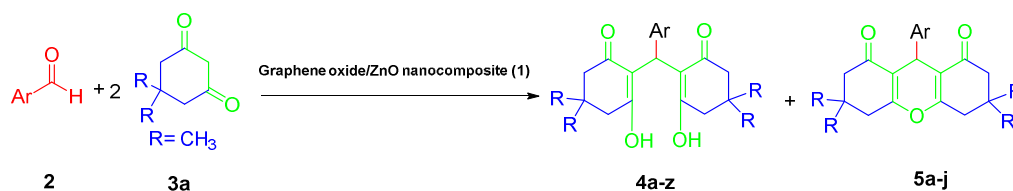
To show the efficiency of the GO/ZnO nanomaterials (**1**), as a catalyst, for the synthesis of tetraketones **4** and xanthenediones **5**, the reaction of 4-chlorobenzaldehyde (**2a**, 1 mmol), and dimedone (**3a**) was investigated as the model reaction. The reaction conditions were optimized with regard to appropriate catalyst loading, different solvents and temperature. The results are summarized in Table 1.

It is noteworthy that the 2,2'-(4-chlorophenyl)methylene bis(3-hydroxy-5,5-dimethyl-2-cyclohexene-1-one) (**4a**) was obtained in very low yields and longer reaction times in the absence of any catalyst even at 90 °C (entries 1,2). Interestingly, after addition of 10 mg of the catalyst (**1**), the yield of the desired tetraketone **4a** in the presence of GO/ZnO nanocomposite (**1**) was significantly improved in shorter reaction time in EtOH under reflux conditions compared to catalyst-free conditions. In the next step, the effect of various solvents such as THF, CH₂Cl₂, CH₃CN and H₂O on the yield and reaction time was studied. The best results, in terms of reaction time and yield of the desired product **4a**, was obtained when the reaction was performed in protic solvents such as EtOH or H₂O (Table 1, entries 3-7). When H₂O was used as the solvent, it afforded the corresponding tetraketone **4a** in 99 % yield and shorter reaction time compared to EtOH. Afterwards, the effect of catalyst loading on the completion of the reaction was examined in the next experiments.

By reducing of the amount of the catalyst to 5 mg catalyst loading, lower yield of the product **4a** was obtained under similar conditions (entry 8). In contrast, increasing of the

amount of the catalyst to 15 mg catalyst loading, had no significant influence on the yield of the desired product (entry 9). On the other hand, both bulk ZnO and GO were also employed, as the catalyst, in the model reaction under similar reaction conditions. It was observed that the desired product **4a** was obtained in lower yields and longer reaction times compared to GO/ZnO nanomaterials (**1**) (Table 1, entries 10 and 11).

Furthermore, the model reaction afforded low yield of the desired product **4a** under ultrasonic conditions at room temperature compared to reflux conditions (entry 12). Finally, when 4-chlorobenzaldehyde **2a** was reacted with dimedone **3a** in the presence of GO/ZnO nanocomposite (**1**) under catalyst-free and solvent-free conditions at 100°C, only 30 % tetraketone **4a** was obtained and no corresponding xanthenedione products **5a** was formed (entry 14). However, after adding of the catalyst to the reaction mixture, only corresponding xanthenedione product **5a** was obtained in excellent yield and shorter reaction time under similar conditions (entry 15). Further increasing of temperature had no remarkable effect on the yield of the desired product **5a** (entries 16 and 17). On the other hand, decreasing of the amount of catalyst loading afforded product **5a** in lower yield and longer reaction time (entry 18). In contrast, increasing of the amount of catalyst to 15 mg catalyst loading had no significant effect on the yield and reaction time (entry 19). Finally, the optimized conditions worked very well for larger scales (5 mmol) of the limiting reactants of both model reactions to afford desired products **4a** and **5a** in high yields, respectively (entries 13 and 20).

Table 1. Optimization of the pseudo three-component reaction 4-chlorobenzaldehyde (**2a**), dimedone (**3a**) under different conditions^a

Entry	Catalyst loading (mg)	Solvent	Temp. (°C)	Time (min)	Yield ^b 4a (%)	Yield ^b 5a (%)
1	-	H ₂ O	r.t	600	40	-
2	-	H ₂ O	90 °C	210	50	-
3	10	EtOH	Reflux	20	95	-
4	10	THF	Reflux	130	70	-
5	10	CH ₂ Cl ₂	Reflux	180	54	-
6	10	MeCN	Reflux	40	80	-
7	10	H ₂ O	Reflux	10	99	-
8	5	H ₂ O	Reflux	10	93	-
9	15	H ₂ O	Reflux	10	99	-
10 ^c	10	H ₂ O	Reflux	240	60	-
11 ^d	10	H ₂ O	Reflux	180	65	-
12 ^e	10	H ₂ O	r.t	60	60	-
13 ^f	50	H ₂ O	Reflux	12	95	-
14	-	Solvent-Free	100	100	30	-
15	10	Solvent-Free	100	30	-	99
16	10	Solvent-Free	110	30	-	99
17	10	Solvent-Free	120	25	-	99
18	5	Solvent-Free	100	30	-	89
19	15	Solvent-Free	100	30	-	99
20 ^f	50	Solvent-Free	100	35	-	93

^a Reaction conditions: 4-chlorobenzaldehyde (**2a**, 1 mmol), dimedone (**3a**, 2 mmol) under different conditions. ^b Isolated yields. ^c Catalysed by ZnO nanoparticles, ^d Catalysed by GO, ^e Under ultrasonic condition. ^f 4-Chlorobenzaldehyde (**2a**, 5 mmol), dimedone (**3a**, 10 mmol).

After finding of optimal conditions, to evaluate the catalytic activity of GO/ZnO nanocomposite (**1**), for the synthesis of tetraketone derivatives, the optimized conditions were further developed to other aromatic carbocyclic and heterocyclic aldehydes **2a-p**. The results are outlined in Table 2. As it can be seen, in all studied examples, good to excellent yields of the desired products **4a-z** were obtained under the optimal reaction conditions within short reaction times. Furthermore, the optimized conditions were also used for the synthesis of xanthenedione derivatives which the results of this part of our study are shown in Table 3. Both aromatic carbocyclic and heterocyclic aldehydes containing electron-withdrawing and electron-donating groups involved in the optimized reaction conditions. The obtained results indicated that the yield of the

reactions is dependent on the substituent effect. In fact, substrates having an electron-withdrawing group on the phenyl ring of aldehydes (Table 2, entries 1-14) produced higher yields of desired products **4** or **5** in same reaction times compared with ones having an electron-donating substituent (Table 2, entries 17-23). Furthermore, heterocyclic aldehydes such as cinamaldehyde (**2n**), furfural (**2o**) and thiophene-2-carbaldehyde (**2p**), which are susceptible to polymerization under acidic conditions, reacted under optimal reaction conditions to afford the corresponding products (Table 2, entries 24-26).

A probable mechanistic pathway for the formation of tetraketones **4** and 1,8-dioxo-octahydroxanthenes **5** is outlined in

Scheme 2. According to the depicted mechanism, it can be proposed that GO/ZnO nanocomposite (**1**) owing to having Lewis and Bronsted acidic sites acts as an acidic catalyst. Therefore, supported Zn (II) species and OH groups on the surface of the catalyst (**1**) can activate the carbonyl group of aldehydes **2** to facilitate nucleophilic addition of dimedone or cyclohexanedione (**3a-b**) on the aldehydes to afford Knoevenagel intermediate (**I**) with elimination of a water molecule. The catalyst can also activate carbonyl group of dimedone or cyclohexanedione (**3a-b**) and is able to increase concentration of the enol form of 1,3-dicarbonyl compounds **3a'-b'**. After that, by Michael addition of second molecule of 1,3-dicarbonyl compounds **3a'-b'** in the second step, tetraketones **4a-z** can be prepared. Finally, ring closure and subsequent tautomerization of the obtained tetraketones and elimination of second molecule of water, in the presence of GO/ZnO nanocomposite (**1**) affords the desired products **5a-j** under solvent-free conditions (Scheme 2). Indeed, effective catalytic activity of GO/ZnO nanocomposite (**1**) compared to other catalysts containing GO structure can be attributed to active Lewis acidic centers.

Another important aspect of this active, efficient, and eco-friendly heterogeneous nanocatalyst is its recyclability. After completion of the reaction, GO/ZnO nanocomposite (**1**) was separated and washed by EtOH, EtOAc and acetone, respectively. The recycled catalyst was then dried under vacuum and reused in subsequent runs. The results are summarized in (Fig. 7). As a part of our study, it has been presented that the GO/ZnO nanocomposites (**1**) could be recovered and reused at least four times in the subsequent runs for the model reaction using the same recovered catalyst without a considerable loss of its catalytic activity.

Table 4 compares the efficiency of GO/ZnO nanocomposite (**1**) with some of the previously introduced procedures to demonstrate its catalytic activity for the synthesis of different tetraketones or 1,8-dioxo-octahydroxanthenes. Obviously, GO/ZnO nanocomposite shows higher catalytic activity in

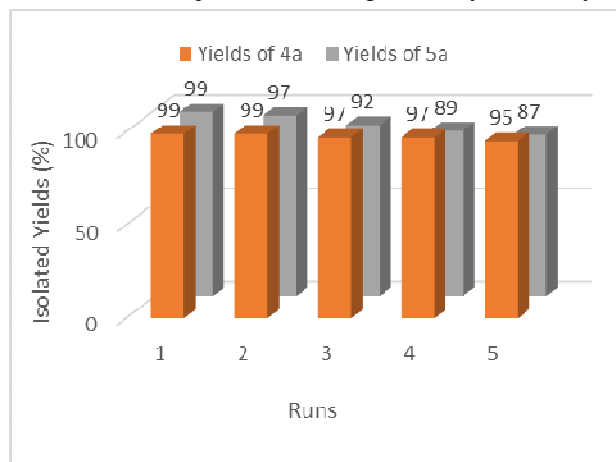
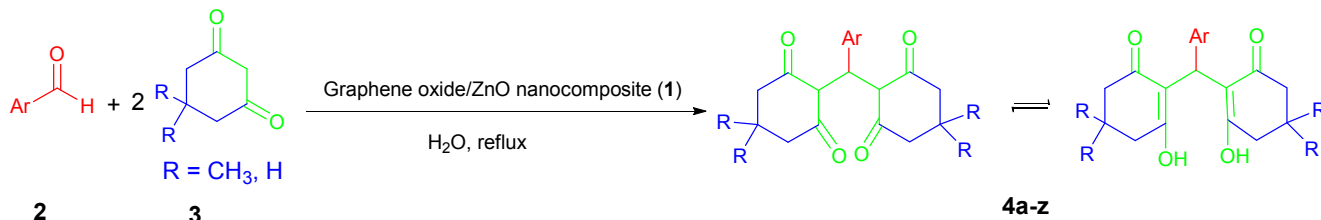
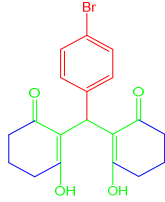
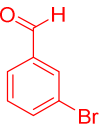
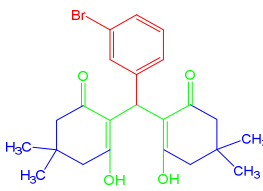
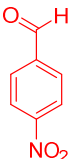
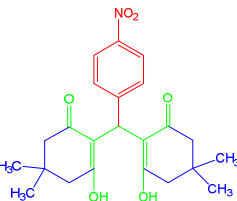
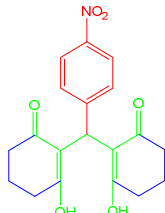
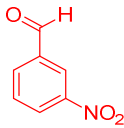
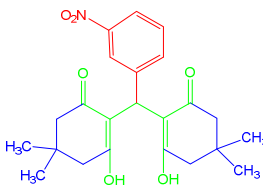
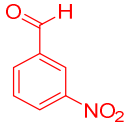
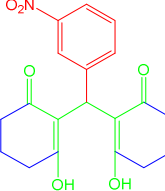


Fig. 7 Reusability of GO/ZnO nanocomposite (**1**) for the synthesis of **4a** and **5a**.

comparison to several of the others in terms of catalyst loading, product yield, avoiding the use of toxic transition metals, toxic solvents and required reaction time.

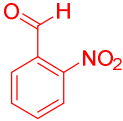
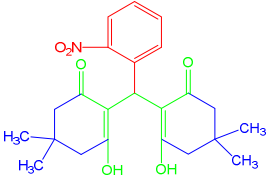
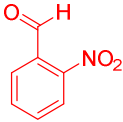
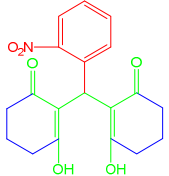
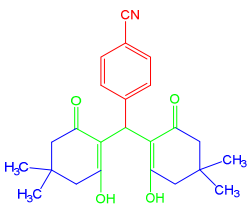
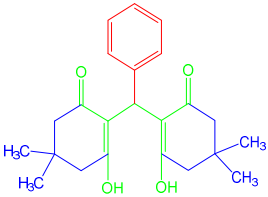
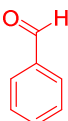
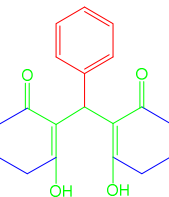
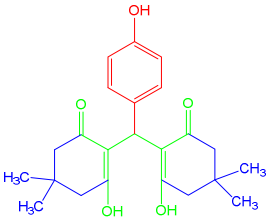
Table 2. GO/ZnO (1) catalyzed one-pot pseudo three-component synthesis of 2,2'-arylmethylene bis(3-hydroxy-5,5-dimethyl-2-cyclohexene-1-one) derivatives **4a-z** from aldehydes **2a-p**, cyclohexanediones **3a-b** under the optimized conditions.^a

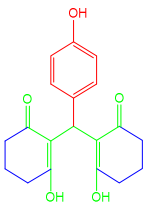
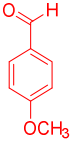
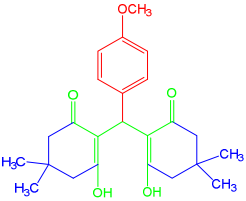
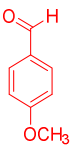
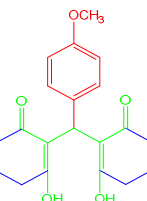
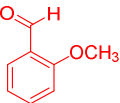
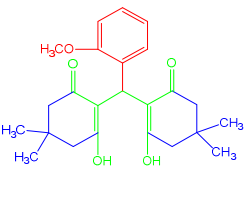
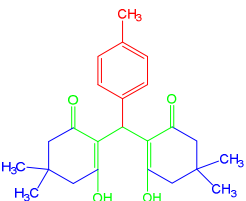
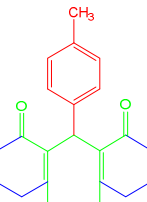
Entry	Aldehyde 2	R	Product 4	Time (min)	Yield ^b (%)	M.p (°C)
						Found / Reported
1		CH ₃		10	99	145/ 140-142 ⁷⁶
2		H		15	96	204/204-206 ⁵⁹
3		CH ₃		10	95	200/ 205 ⁷⁷
4		H		15	94	227/229-231 ⁵⁹
5		CH ₃		10	96	154/158-159 ⁷⁸

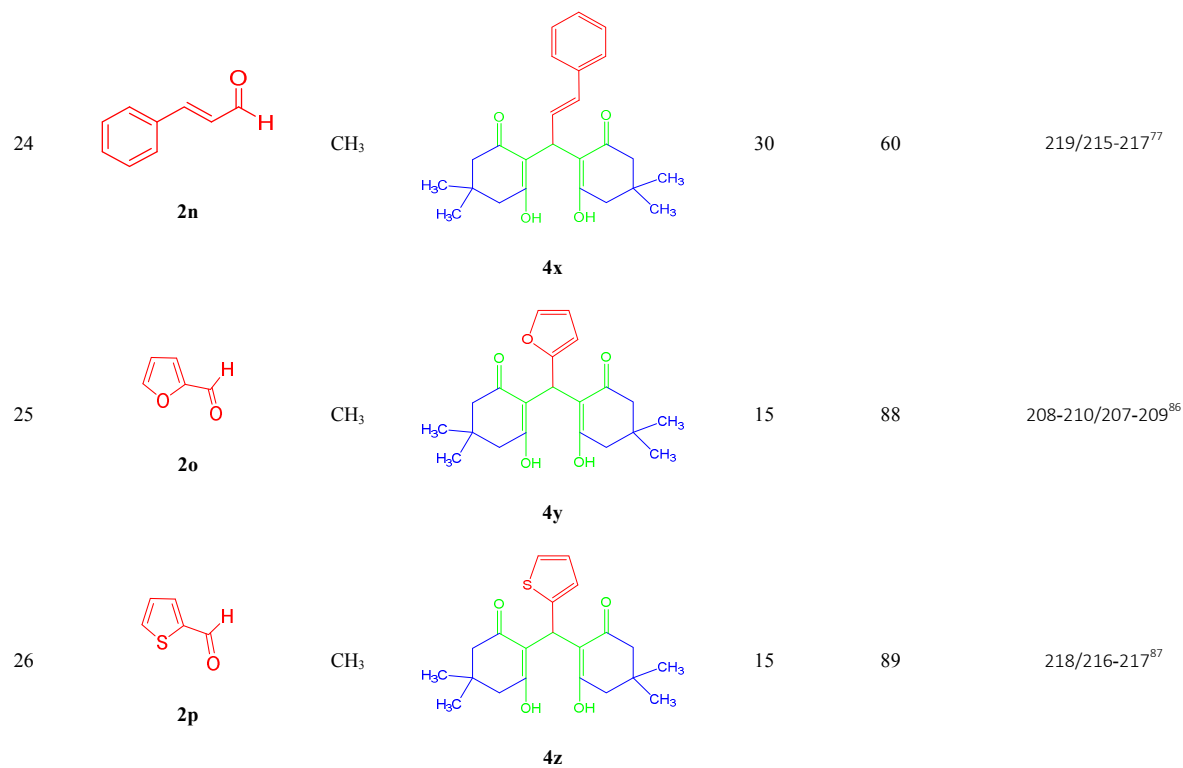
6	<p>2c</p>  <p>2c</p>	H	<p>4e</p>  <p>4e</p>	15	90	243/240-241 ⁷⁹
7	<p>2c</p>  <p>2c</p>	CH ₃	<p>4f</p>  <p>4f</p>	10	96	204/201-203 ⁴⁹
8	<p>2d</p>  <p>2d</p>	CH ₃	<p>4g</p>  <p>4g</p>	10	97	192/188-190 ⁸⁰
9	<p>2e</p>  <p>2e</p>	H	<p>4h</p>  <p>4h</p>	15	95	217/218 ⁸¹
10	<p>2e</p>  <p>2e</p>	CH ₃	<p>4i</p>  <p>4i</p>	10	95	199/197-198 ⁷⁷
11	<p>2f</p>  <p>2f</p>	H	<p>4j</p>  <p>4j</p>	15	92	207/209-210 ⁸²

ARTICLE

New J. Chem.

12		CH ₃		10	96	192/188-190 ⁵⁸
	2g		4l			
13		H		15	91	213/212-213 ⁸²
	2g		4m			
14		CH ₃		10	97	169-171/165-167 ⁸³
	2h		4n			
15		CH ₃		10	95	196 / 194-195 ⁷⁷
	2i		4o			
16		H		15	93	219/217-218 ⁸²
	2i		4p			
17		CH ₃		10	94	188-190/188-190 ⁸³
	2j		4q			

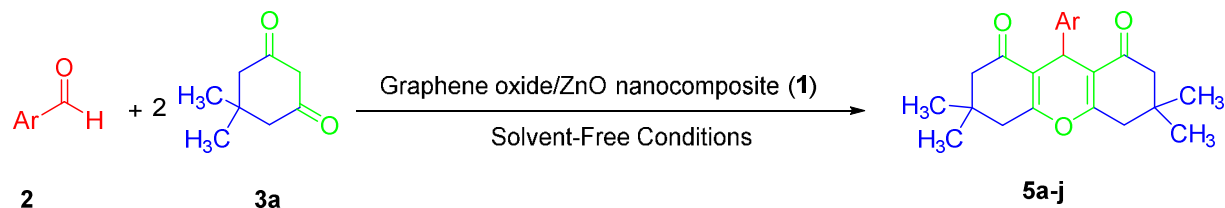
18		H		15	92	196/192-194 ⁵⁹
	2j		4r			
19		CH ₃		10	88	145/142-143 ⁸⁴
	2k		4s			
20		H		15	87	197/193-195 ⁵⁹
	2k		4t			
21		CH ₃		10	89	185/187-188 ⁷⁷
	2l		4u			
22		CH ₃		10	85	130/126-128 ⁸⁰
	2m		4v			
23		H		20	82	193/190-191 ⁸⁵
	2m		4w			



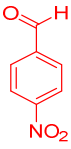
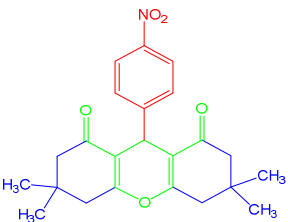
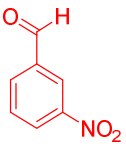
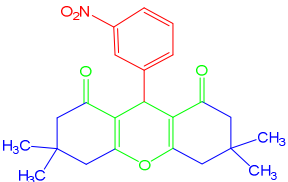
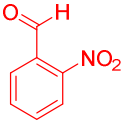
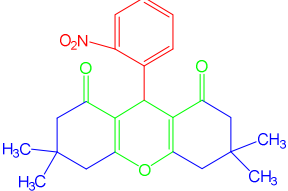
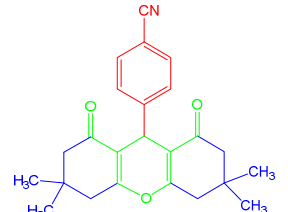
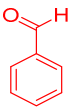
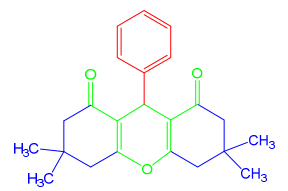
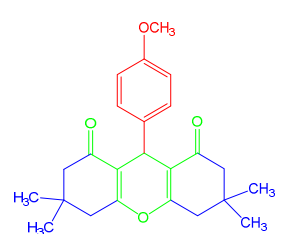
^a Reaction conditions: 4-Chlorobenzaldehyde (**2a**, 1 mmol), dimedone (**3a**, 2 mmol) or 1,3-cyclohexanedione (**3b**, 2 mmol) in the presence of 10 mg of the catalyst (**1**) under H₂O reflux conditions at 100 °C. ^b Isolated Yields.

New J. Chem.

ARTICLE

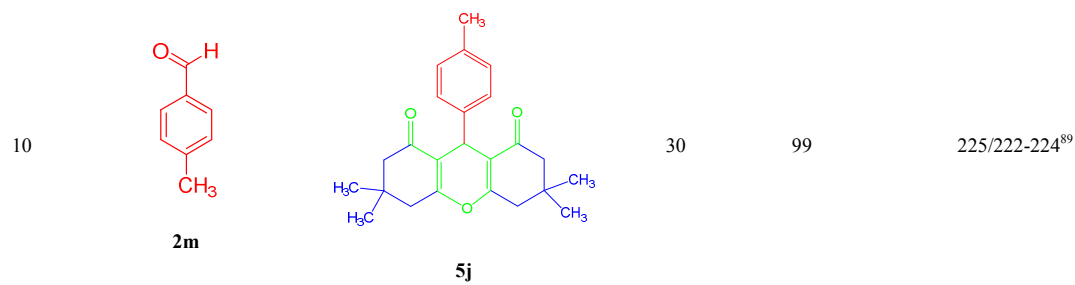
Table 3. GO/ZnO (**1**) catalyzed one-pot pseudo three-component synthesis of 1,8-dioxo-octahydroxanthenes **5a** from aldehydes **2**, dimedone (**3a**) under the optimized conditions.^a

Entry	Aldehyde 2	Product 5	Time (min)	Yield ^b (%)	M.p (°C)
					Found / Reported
1			30	99	231-233/ 230-233 ⁸⁸
2			40	89	223-225/226-228 ⁸⁹
3			30	90	240-242/ 242-244 ⁹⁰

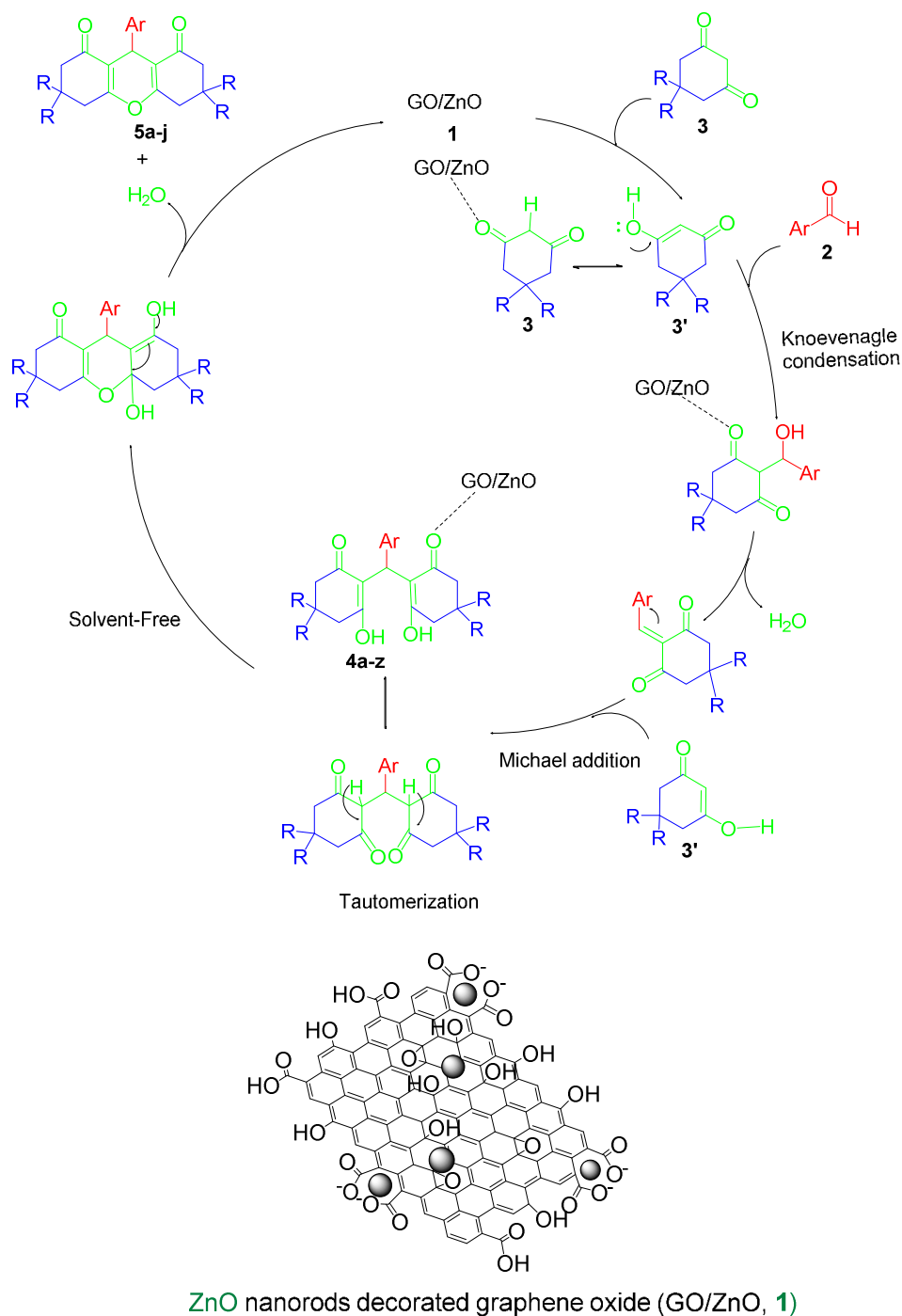
4	 <p>2e</p>	 <p>5d</p>	30	92	228/224-226 ⁹⁰
5	 <p>2f</p>	 <p>5e</p>	40	90	167-169/164-166 ⁹⁰
6	 <p>2g</p>	 <p>5f</p>	40	90	256/258-262 ⁹¹
7	 <p>2h</p>	 <p>5g</p>	30	95	224/220-222 ⁹⁰
8	 <p>2i</p>	 <p>5h</p>	45	91	200/199-200 ⁹²
9	 <p>2k</p>	 <p>5i</p>	40	92	246/241-243 ⁹³

New J. Chem.

ARTICLE



^a Reaction conditions: 4-chlorobenzaldehyde (**2a**, 1 mmol), dimedone (**3a**, 2 mmol) in the presence of 10 mg of the catalyst (**1**) under solvent-free conditions at 100 °C. ^b Isolated Yields.



ZnO nanorods decorated graphene oxide (GO/ZnO, **1**)

Scheme 2. Proposed mechanism for the synthesis of tetraketones **4** and 1,8-dioxo-octahydroxanthenes **5** catalyzed by GO/ZnO nanocomposite (**1**).

Table 4. Comparative synthesis of compounds **4a** and **5a** using the reported methods versus the present method.

Entry	Catalyst	Catalyst Loading	Solvent	Temp (°C)	Time (min)	Yield (%) 4a	Yield (%) 5a	Ref.
1	G-SO ₃ H	20 mg	H ₂ O	80	120	-	90	61
2	GO	20 mg	H ₂ O	80	120	-	81	61
3	Nanocrystalline TiO ₂	10 mg	Neat	80	23	-	95	45
4	Natural phosphate	500 mg	H ₂ O	rt	120	98	-	51
5	Natural phosphate	1500 mg	EtOH (90%)	78	390	-	90	51
6	Fe ₃ O ₄ @SiO ₂ -Imid-PMA	30 mg	EtOH	78	60	-	91	53
7	Copper (0) nanoparticles onto silica	100 mg	EtOH	80	60	93	-	46
8	CoFe ₂ O ₄ nanoparticles	11.7 mg	H ₂ O : EtOH (1 : 1)	60	4	89	-	59
9	Fe ₃ O ₄ @SiO ₂ -SO ₃ H	10 mg	H ₂ O	rt	80	83	-	94
10	Nano Fe/NaY zeolite	2.5 mg	EtOH	78	70	98	-	95
12	GO/ZnO	10 mg	H ₂ O	100	10	99	-	This Work
13	GO/ZnO	10 mg	Neat	100	30	-	99	This Work

Experimental

General

All chemicals were purchased from Merck or Aldrich companies and were used as received. Field emission scanning electron microscopy (FESEM) images and Energy dispersive spectroscopy (EDX) patterns was obtained using MIRA III instrument of TESCAN Company, Czech Republic. Thermal gravimetric analysis (TGA) was performed by means of Netzsch -TGA 209 F1 instrument. X-Ray diffraction patterns (XRD) was obtained using PW1730 instrument of PHILIPS Company. FTIR spectra were acquired as KBr pellets on a Shimadzu FTIR-8400S spectrometer. Melting points were determined using an Electrothermal 9100 apparatus and are uncorrected. ¹H NMR (500 MHz) spectra were recorded using a INOVA-500 spectrometer in CDCl₃, as solvent, at ambient temperature. Analytical thin layer chromatography (TLC) for monitoring reactions was carried out using Merck 0.2 mm silica gel 60 F-254 Al-plates using EtOAc and n-hexane as eluents.

General procedure for the preparation of GO

Graphene oxide (GO) was made by a modified Hummers method using graphite flake as starting material.⁷⁴ Graphite flake (1 g) was stirred with NaNO₃ (0.5 g) in 98% H₂SO₄ (23

mL) for 120 min in an oil bath at 65 °C. Then KMnO₄ (3 g) was gradually added while keeping the temperature <20 °C. The mixture was then stirred at 35-40 °C for 30 min and at 65-80 °C for 45 min, respectively. Next, distilled water (46 mL) was added and the mixture heated at 98-105 °C for 30 min. The reaction was terminated by addition of distilled water (140 mL) and 30% H₂O₂ solution (10 mL). The obtained solid was washed by repeated centrifugation and filtration, first with 5% HCl aqueous solution, and then distilled water. Water (160 mL) was added to the final product and dried at 70 °C in an oven for 2 days.

General procedure for the preparation of GO/ZnO nanocomposite (1)

GO/ZnO nanocomposite (**1**) was prepared with weight ratio of (1:1) between GO and ZnO. 1 g dried GO was dispersed in 100 mL of water and sonicated for 1 h to achieve a well dispersed suspension. Then, 1.1 g of zinc acetate (Zn(CH₃CO₂)₂ · 2H₂O) was dissolved in 20 mL deionized water and added to suspension. The obtained mixture was sonicated for 10 min and then definite amount of NaOH (1 M) was successively added slowly to the above GO suspension until its pH reach 7.0 and subsequently followed by sonication for 30 min. Then the mixture was stirred at 70 °C for 12 h. Finally, the composite was centrifuged and

ARTICLE

New J. Chem.

washed several times with deionized water and the obtained materials was dried at 70 °C.

General experimental procedure for the synthesis of 2,2'-arylmethylene bis(3-hydroxy-5,5-dimethyl-2-cyclohexene-1-one) derivatives (4a-z)

In a 5 mL round-bottomed flask, aldehyde (**2**, 1 mmol), 1,3-dicarbonyl compound (**3**, 2 mmol) and GO/ZnO (**1**, 10 mg) were added to H₂O (5 mL). The obtained mixture was stirred under reflux conditions for times indicated in Table 2 to afford products (**4a-z**). The reaction progress was monitored by TLC (eluent: n-Hexane:EtOAc, 10:1). After completion of the reaction, water was evaporated and hot EtOH (5 mL) was added to the solid mixture and stirred. Then the catalyst was separated by centrifuging followed by filtration. The filtrate was kept at ambient temperature to afford desired products **4a-z**. The obtained products were characterized by measuring of their melting point as well as FTIR and ¹H NMR spectroscopy.

General experimental procedure for the synthesis of 1,8-dioxo-octahydroxanthenes (5a-j)

To a mixture of aromatic aldehyde (**2**, 1 mmol) and 1,3-dicarbonyl compound (**3**, 2 mmol), 10 mg GO/ZnO was added and then the reaction mixture was stirred at 100 °C. The progress of reaction was monitored by TLC (eluent: n-Hexane:EtOAc, 10:5). After completion of the reaction, hot EtOH (5 mL) was added to the solid mixture and centrifuged to separate the catalyst before its filtration. The filtrate was kept at ambient temperature to afford desired products (**5a-j**). The structure of the products was identified by measuring of their melting point as well as FTIR and ¹H NMR spectroscopy.

Conclusions

In conclusion, we have developed a mild, simple and efficient methodology for the synthesis of 2,2'-arylmethylene bis(3-hydroxy-5,5-dimethyl-2-cyclohexene-1-one) and 1,8-dioxo-1,2,3,4,5,6,7,8-octahydroxanthene derivatives using highly effective and recyclable ZnO nanorods decorated graphene oxide (GO/ZnO) nanocomposite. The desired products were produced in good to excellent yields and short reaction times in the present protocol. High to excellent yields, low loading of the catalyst, eliminating of any toxic solvent, easy separation and purification of the products as well as reusability of the catalyst are the most significant advantages of this protocol.

Acknowledgements

We are grateful for the financial support from The Research Council of Iran University of Science and Technology (IUST), Tehran, Iran (Grant No 160/347). We would also like to acknowledge the support of The Iran Nanotechnology Initiative Council (INIC), Iran.

Notes and references

1. A. P. Dowling, *Materials Today*, 2004, **7**, 30-35.
2. D. V. Talapin and E. V. Shevchenko, *Chemical Reviews*, 2016, **116**, 10343-10345.
3. X. Qien, S. Yuanhui, L. Yihong and L. Zhe, *Current Organic Chemistry*, 2016, **20**, 2013-2021.
4. S. Hasan, *A Review on Nanoparticles: Their Synthesis and Types*, 2015.
5. V. Polshettiwar and R. S. Varma, *Green Chemistry*, 2010, **12**, 743-754.
6. N. Hashim, Z. Muda, M. Z. Hussein, I. M. Isa, A. Mohamed, A. Kamari, S. A. Bakar, M. Mamat and A. Jaafar, *J. Mater. Environ. Sci.*, 2016, **7**, 3225-3243.
7. M. Khan, M. N. Tahir, S. F. Adil, H. U. Khan, M. R. H. Siddiqui, A. A. Al-warthan and W. Tremel, *Journal of Materials Chemistry A*, 2015, **3**, 18753-18808.
8. T. Yumura and A. Yamasaki, *Physical Chemistry Chemical Physics*, 2014, **16**, 9656-9666.
9. M. Supur, Y. Kawashima, K. Ohkubo, H. Sakai, T. Hasobe and S. Fukuzumi, *Physical Chemistry Chemical Physics*, 2015, **17**, 15732-15738.
10. M. Ishani, M. G. Dekamin and Z. Alirezvani, *Journal of Colloid and Interface Science*, 2018, **521**, 232-241.
11. Y. Zhu, S. Murali, W. Cai, X. Li, J. W. Suk, J. R. Potts and R. S. Ruoff, *Advanced materials*, 2010, **22**, 3906-3924.
12. X. Sun, Z. Liu, K. Welscher, J. T. Robinson, A. Goodwin, S. Zaric and H. Dai, *Nano research*, 2008, **1**, 203-212.
13. X. Dong, W. Huang and P. Chen, *Nanoscale Res Lett*, 2010, **6**, 60.
14. H. Sun, L. Cao and L. Lu, *Nano Research*, 2011, **4**, 550-562.
15. N. Kausar, P. Mukherjee and A. R. Das, *RSC Advances*, 2016, **6**, 88904-88910.
16. W. Liu, *Chemical Engineering Science*, 2007, **62**, 3502-3512.
17. A. B. Djuricic, X. Chen, Y. H. Leung and A. Man Ching Ng, *Journal of Materials Chemistry*, 2012, **22**, 6526-6535.
18. A. Hatamie, A. Khan, M. Golabi, A. P. F. Turner, V. Beni, W. C. Mak, A. Sadollahkhani, H. Alnoor, B. Zargar, S. Bano, O. Nur and M. Willander, *Langmuir*, 2015, **31**, 10913-10921.
19. P. Rajagopalan, S. Vipul and I. A. Palani, *Nanotechnology*, 2018, **29**, 105406.
20. M. Ibrahim Dar, N. Arora, N. Pratap Singh, S. Sampath and S. A. Shivashankar, *New Journal of Chemistry*, 2014, **38**, 4783-4790.
21. X. Cai, B. Han, S. Deng, Y. Wang, C. Dong, Y. Wang and I. Djerdj, *CrystEngComm*, 2014, **16**, 7761-7770.
22. Z. L. Wang, *Materials Today*, 2004, **7**, 26-33.
23. F. Xu and L. Sun, *Energy & Environmental Science*, 2011, **4**, 818-841.
24. C. Mondal, M. Ganguly, A. K. Sinha, J. Pal and T. Pal, *RSC Advances*, 2013, **3**, 5937-5944.
25. B. J. Kim, M. W. Kim, J. S. Jang and E. A. Stach, *Nanoscale*, 2014, **6**, 6984-6990.
26. H. Sharma, N. Kaur, N. Singh and D. O. Jang, *Green Chemistry*, 2015, **17**, 4263-4270.
27. L. K. M., K. K. B. Shiva and S. Ch., *Advanced Synthesis & Catalysis*, 2005, **347**, 1212-1214.
28. Z. Mirjafary, H. Saeidian, A. Sadeghi and F. M. Moghaddam, *Catalysis Communications*, 2008, **9**, 299-306.
29. J. Safaei-Ghomi and M. A. Ghasemzadeh, *Chinese Chemical Letters*, 2012, **23**, 1225-1229.
30. S. Banerjee, S. Payra, A. Saha and G. Sereda, *Tetrahedron Letters*, 2014, **55**, 5515-5520.
31. M. Nasrollahzadeh, B. Jaleh and A. Jabbari, *RSC Advances*, 2014, **4**, 36713-36720.
32. V. Galstyan, E. Comini, I. Kholmanov, G. Faglia and G. Sberveglieri, *RSC Advances*, 2016, **6**, 34225-34232.
33. S. Mathialagan, G. Ponnaiah and M. Vijay, 2017.
34. F. Ghoreishi, V. Ahmadi and M. Samadpour, *Journal of Nanostructures*, 2013, **3**, 453-459.

35. L. Huang, Y. Zhang, H. Liu, B. Liu and M. Tu, *New Journal of Chemistry*, 2014, **38**, 5817-5824.
36. R. A. Rakkesh, D. Durgalakshmi and S. Balakumar, *RSC Advances*, 2016, **6**, 34342-34349.
37. G. M. Maharvi, S. Ali, N. Riaz, N. Afza, A. Malik, M. Ashraf, L. Iqbal and M. Lateef, *Journal of Enzyme Inhibition and Medicinal Chemistry*, 2008, **23**, 62-69.
38. K. M. Khan, G. M. Maharvi, M. T. H. Khan, A. Jabbar Shaikh, S. Perveen, S. Begum and M. I. Choudhary, *Bioorganic & Medicinal Chemistry*, 2006, **14**, 344-351.
39. K. M. Khan, G. M. Maharvi, M. T. H. Khan, A. J. Shaikh, S. Perveen, S. Begum and M. I. Choudhary, *Bioorganic & medicinal chemistry*, 2006, **14**, 344-351.
40. A. A. Napoleon and F.-R. N. Khan, *Medicinal Chemistry Research*, 2014, **23**, 4749-4760.
41. R. Singla, K. B. Gupta, S. Upadhyay, M. Dhiman and V. Jaitak, *Bioorganic & Medicinal Chemistry*, 2018, **26**, 266-277.
42. M. Saha and A. K. Pal, *Tetrahedron Letters*, 2011, **52**, 4872-4877.
43. J. Griffiths and W. J. Lee, *Dyes and Pigments*, 2003, **57**, 107-114.
44. J. M. KHURANA and K. VIJ, *Journal of Chemical Sciences*, 2012, **124**, 907-912.
45. E. Eidi, M. Z. Kassaei and Z. Nasresfahani, *Applied Organometallic Chemistry*, 2015, **29**, 793-797.
46. M. GUPTA and M. GUPTA, *Journal of Chemical Sciences*, 2016, **128**, 849-854.
47. P. J. Das and J. Das, *RSC Advances*, 2015, **5**, 11745-11752.
48. B. Karami, Z. Zare and K. Eskandari, *Chemical Papers*, 2013, **67**, 145-154.
49. B. M. Sapkal, P. K. Labhane and J. R. Satam, *Research on Chemical Intermediates*, 2017, **43**, 4967-4979.
50. K. P. Nandre, V. S. Patil and S. V. Bhosale, *Chinese Chemical Letters*, 2011, **22**, 777-780.
51. A. Fallah, M. Tajbakhsh, H. Vahedi and A. Bekhradnia, *Research on Chemical Intermediates*, 2017, **43**, 29-43.
52. L. Jiang, B. Wang, R.-R. Li, S. Shen, H.-W. Yu and L.-D. Ye, *Chinese Chemical Letters*, 2014, **25**, 1190-1192.
53. K. Gong, H. Wang, S. Wang, Y. Wang and J. Chen, *Chinese Journal of Catalysis*, 2015, **36**, 1249-1255.
54. S. Rostamizadeh, A. M. Amani, G. H. Mahdavinia, G. Amiri and H. Sepehrian, *Ultrasonics Sonochemistry*, 2010, **17**, 306-309.
55. M. A. Zolfigol, R. Ayazi-Nasrabadi, S. Bagheri, V. Khakyzadeh and S. Azizian, *Journal of Molecular Catalysis A: Chemical*, 2016, **418-419**, 54-67.
56. A. Thakur, A. Sharma and A. Sharma, *Synthetic Communications*, 2016, **46**, 1766-1771.
57. M. Ahmad, T. A. King, D.-K. Ko, B. H. Cha and J. Lee, *Journal of Physics D: Applied Physics*, 2002, **35**, 1473.
58. Y. Ren, B. Yang and X. Liao, *RSC Advances*, 2016, **6**, 22034-22042.
59. J. K. Rajput and G. Kaur, *Catalysis Science & Technology*, 2014, **4**, 142-151.
60. Z. Lasemi and E. Mehrafsbi, *Research on Chemical Intermediates*, 2015, **41**, 2855-2866.
61. A. Shaabani, M. Mahyari and F. Hajishaabanha, *Research on Chemical Intermediates*, 2014, **40**, 2799-2810.
62. J.-T. Li, Y.-W. Li, Y.-L. Song and G.-F. Chen, *Ultrasonics Sonochemistry*, 2012, **19**, 1-4.
63. M. G. Dekamin, F. Mehdipoor and A. Yaghoubi, *New Journal of Chemistry*, 2017, **41**, 6893-6901.
64. M. G. Dekamin, M. Azimoshan and L. Ramezani, *Green Chemistry*, 2013, **15**, 811-820.
65. M. G. Dekamin, Z. Karimi, Z. Latifidoost, S. Ilkhanizadeh, H. Daemi, M. R. Naimi-Jamal and M. Barikani, *International Journal of Biological Macromolecules*, 2018, **108**, 1273-1280.
66. M. G. Dekamin and M. Eslami, *Green Chemistry*, 2014, **16**, 4914-4921.
67. Y. Amene and D. M. G., *ChemistrySelect*, 2017, **2**, 9236-9243.
68. M. G. Dekamin, E. Arefi and A. Yaghoubi, *RSC Advances*, 2016, **6**, 86982-86988.
69. M. G. Dekamin, S. Z. Peyman, Z. Karimi, S. Javanshir, M. R. Naimi-Jamal and M. Barikani, *International Journal of Biological Macromolecules*, 2016, **87**, 172-179.
70. A. Alinasab Amiri, S. Javanshir, Z. Dolatkhan and M. G. Dekamin, *New Journal of Chemistry*, 2015, **39**, 9665-9671.
71. M. G. Dekamin and S. Z. Peyman, *Monatshefte für Chemie - Chemical Monthly*, 2016, **147**, 445-450.
72. A. Yaghoubi, M. G. Dekamin and B. Karimi, *Catalysis Letters*, 2017, **147**, 2656-2663.
73. A. Yaghoubi, M. G. Dekamin, E. Arefi and B. Karimi, *Journal of Colloid and Interface Science*, 2017, **505**, 956-963.
74. W. S. Hummers and R. E. Offeman, *Journal of the American Chemical Society*, 1958, **80**, 1339-1339.
75. Y.-L. Chen, C.-E. Zhang, C. Deng, P. Fei, M. Zhong and B.-T. Su, *Chinese Chemical Letters*, 2013, **24**, 518-520.
76. S. Kantevari, R. Bantu and L. Nagarapu, *Journal of Molecular Catalysis A: Chemical*, 2007, **269**, 53-57.
77. E. Horning and M. Horning, *The Journal of organic chemistry*, 1946, **11**, 95-99.
78. F. Darviche, S. Balalaie, F. Chadegani and P. Salehi, *Synthetic Communications*, 2007, **37**, 1059-1066.
79. J. M. Khurana and K. Vij, *Journal of Chemical Sciences*, 2012, 1-6.
80. D. Shi, Y. Wang, Z. Lu and G. Dai, *Synthetic Communications*, 2000, **30**, 713-726.
81. F. King and D. Felton, *Journal of the Chemical Society*, 1948, 1371-1372.
82. F. E. King and D. G. I. Felton, *Journal of the Chemical Society (Resumed)*, 1948, DOI: 10.1039/JR9480001371, 1371-1372.
83. F. Darviche, S. Balalaie, F. Chadegani and P. Salehi, *Synthetic Communications*, 2007, **37**, 1059-1066.
84. T. S. Jin, J. S. Zhang, A. Q. Wang and T. S. Li, *Synthetic Communications*, 2005, **35**, 2339-2345.
85. V. K. Rao, M. M. Kumar and A. Kumar, 2011.
86. Y. Zhang and Z. Shang, *Chinese Journal of Chemistry*, 2010, **28**, 1184-1188.
87. R. Sedghi, M. M. Heravi, S. Asadi, N. Nazari and M. R. Nabid, *Current Organic Chemistry*, 2016, **20**, 696-734.
88. G. Song, B. Wang, H. Luo and L. Yang, *Catalysis Communications*, 2007, **8**, 673-676.
89. M. Rahimifard, G. Mohammadi Ziarani, A. Badiei, S. Asadi and A. Abolhasani Soorki, *Research on Chemical Intermediates*, 2016, **42**, 3847-3861.
90. M. A. Zolfigol, V. Khakyzadeh, A. R. Moosavi-Zare, A. Zare, S. B. Azimi, Z. Asgari and A. Hasaninejad, *Comptes Rendus Chimie*, 2012, **15**, 719-736.
91. R. Kazemi-Rad, J. Azizian and H. Kefayati, *Journal of the Chinese Chemical Society*, 2015, **62**, 311-315.
92. E. Mosaddegh, M. R. Islami and A. Hassankhani, *Arabian Journal of Chemistry*, 2012, **5**, 77-80.
93. X. Fan, X. Hu, X. Zhang and J. Wang, *Canadian journal of chemistry*, 2005, **83**, 16-20.
94. F. Nemati, M. M. Heravi and R. Saeedi Rad, *Chinese Journal of Catalysis*, 2012, **33**, 1825-1831.
95. M. Tajbakhsh, M. Heidary and R. Hosseinzadeh, *Research on Chemical Intermediates*, 2016, **42**, 1425-1439.

Graphical Abstract

